Regional Characterization of Activation Times in Spontaneous and Drug-Induced Brugada Syndrome Using ECG Imaging

Inés Noguero-Soler[1], Isabel Montilla-Padilla[2], Javier Ramos-Maqueda[2], Esther Pueyo[1,3], Ana Mincholé[1,3]

[1] BSICoS, I3A, IIS Aragón, University of Zaragoza, Zaragoza, Spain
[2] Clinical Hospital Lozano Blesa, Zaragoza, Spain
[3] CIBER en Bioingeniería, Biomateriales y Nanomedicina (CIBER-BBN), Spain

Abstract

Brugada syndrome (BrS) is a cardiac channelopathy associated with an increased risk of sudden cardiac death. Its diagnosis is based on the presence of a characteristic coved-type electrocardiographic pattern (ST-segment elevation with inverted T wave) in the right precordial leads. This study aims to assess ventricular activation abnormalities in BrS patients using non-invasive electrocardiographic imaging (ECGi), comparing activation profiles of patients with spontaneous (BrS_1) and drug-induced (BrS_2) patterns to those of healthy controls. A cohort of BrS patients and control subjects underwent ECGi analysis to quantify global and regional ventricular activation times (ATs). Global measurements revealed significantly prolonged QRS duration (BrS_1: 134 ±21 ms; BrS_2: 135±18 ms, Healthy: 116±12 ms) and total ventricular ATs (BrS_1: 86±16 ms; BrS_2: 82.9±13.5 ms; Healthy: 67±13 ms) in BrS patients versus controls. Regional analysis showed delayed conduction in the right ventricular outflow track (RVOT) in BrS patients, with additional differences between BrS_1 and BrS_2 in other ventricular regions. These findings indicate that BrS is characterized by delayed conduction, particularly in the RVOT, with distinct activation profiles between spontaneous and induced types, underscoring electrophysiological heterogeneity within the syndrome.

1. Introduction

Brugada Syndrome (BrS) is a rare inherited arrhythmogenic disorder characterized by a distinctive electrocardiographic pattern in the right precordial leads. Affected individuals, typically young adults, face an increased risk of life-threatening ventricular arrhythmias compared with age-matched healthy populations [1]. Pathophysiological studies have revealed conduction delays, particularly in the right ventricular outflow tract (RVOT) epicardium, as well as subtle epicardial and interstitial fibrosis in BrS patients with recurrent ventricular fibrillation.

Clinically, BrS is diagnosed by the presence of a characteristic pattern in the electrocardiogram (ECG) consisting of coved-type ST-segment elevation in the right precordial leads, followed by an inverted T wave. When spontaneous manifestations are absent, the diagnosis is often unmasked by administering sodium channel blockers as ajmaline. However, this pharmacological challenge carries inherent risks, and its diagnostic specificity has been increasingly questioned, with part of the medical community suggesting that a positive ajmaline test alone may be insufficient for a definitive diagnosis [2].

Over the last years, electrocardiographic imaging (ECGi) has emerged as a powerful non-invasive method for investigating the BrS substrate. By solving the inverse problem of electrocardiography, ECGi infers unipolar electrograms (EGMs) on a three-dimensional ventricular geometry from body surface potential mapping (BSPM) signals, thereby enabling region-specific electrophysiological analysis. Pannone et al. [3] employed ECGi during ajmaline testing and identified RVOT activation and repolarization differences between BrS patients with and without sudden cardiac death events. Isbister et al. [4] used ECGi during hydroquinidine administration and showed marked ventricular repolarization abnormalities in BrS patients, particularly within the RVOT. Monaco et al. [5] proposed an RVOT delay with respect to RV threshold of more than 45% to be used for stratification of Right Bundle Branch Block and BrS patients in cases where ECG alone is inconclusive. Despite these advances, how epicardial activation differs between spontaneous and drug-induced BrS patterns remains insufficiently explored.

This work aims to further characterize epicardial activation in BrS patients, encompassing both spontaneous and drug-induced patterns, propose a methodology to estimate activation from complex unipolar electrograms and assess ECGi-derived epicardial activation maps against healthy

controls. These findings may provide new insights into the pathophysiological mechanisms underlying BrS and contribute to improved risk stratification for malignant arrhythmic events.

2. Methods

Study population: ECGi recordings were collected at Hospital Clínico Universitario Lozano Blesa (Zaragoza, Spain) using the Acorys mapping system (Corify Care SL). The study cohort included 18 patients diagnosed with BrS and 9 healthy controls (n=9, 7 male, 40±13 years). Among BrS patients, 9 presented a spontaneous type 1 ECG pattern (hereafter referred to as BrS_1 group, 9 males, 48±11 years), while 11 presented an induced type 1 pattern following ajmaline challenge (hereafter BrS_2 group, 7 males, 58±10 years). Patients with a low Shanghai score [6] were excluded from the induced-pattern group.

BSPM: BSPM signals were recorded using 128 electrodes as patients rested in a supine position during medical consultation. The acquired signals underwent a built-in software pre-filtering, thus requiring no additional preprocessing. Standard 12-lead and high-precordial lead Brugada ECGs were then inferred from the BSPM data. The onset ($QRS_{on,l}$) and the end ($QRS_{end,l}$) of the QRS complex in each lead l were identified using a wavelet-based delineation algorithm [7]. A global QRS onset, QRS_{on}, was defined as the latest $QRS_{on,l}$ mark that fulfilled the condition of being preceded within 12 ms by $QRS_{on,l}$ marks in at least 25% of leads. Similarly, a global QRS end, QRS_{end}, was defined as the latest $QRS_{end,l}$ mark meeting the analogous condition for $QRS_{end,l}$ marks. QRS_w was computed as the time difference between QRS_{on} and QRS_{end}. QRS_{on} was selected as a consistent reference for subsequent activation time (AT) analysis.

EGM reconstruction and AT detection: The ventricular mesh (≈3900 nodes) and corresponding EGMs were retrieved from Acorys software. Heart geometry was estimated by the software from template models using the patients' height and weight. ATs were determined for each EGM as the time associated with the steepest downslope of the most negative deflection within the QRS window. We adapted a wavelet transform-based method from [7] to detect local minima, applying an amplitude-based criterion in the wavelet domain to exclude notches. When two negative deflections showed comparable amplitudes (amplitude ratio>0.4) and the first deflection was initially selected as the steepest negative slope, the activation time was defined as the mean of the timings of the first and second deflections. This approach was proposed to deal with complex EGMs, as considering solely the first deflection in these cases could underestimate the later activation when a pronounced R'was present.

To reduce the impact of AT outliers, neighbor information was incorporated by applying a mild Laplacian smooth.

Total AT: Global first (AT_{first}) and last (AT_{last}) ATs were defined as the earliest and latest ATs across all EGMs. Total activation time (TAT) was measured as the interval between AT_{first} and AT_{last}.

Regional analysis: Ventricular geometries and corresponding homologous segmentations were provided by Acorys software. The ventricles were divided into 15 segments: basal, medial and apical divisions, with the right ventricle (RV) segmented into anterior and posterior regions, and the left ventricle (LV) segmented into anterior, posterior, and lateral regions. Results are displayed using bullseye plot representations, with RV and LV regions arranged according to conventional cardiological orientation, and concentric rings corresponding to basal (outer), medial (middle), and apical (inner) layers. Based on this segmentation, the RVOT was predominantly located within the anterior basal segment of the right ventricle (RVAB), with a smaller portion extending into the anterior medial segment (RVAM).

For each segment, the median AT (AT_m), as well as the 10th (AT_{10}), 25th (AT_{25}) and 90th (AT_{90}) percentiles, were extracted to characterize representative median, minimum, and maximum values.

Statistical analysis: Differences between groups in global and regional markers were assessed using the unpaired Wilkonson rank-sum test. Statistical significance was defined as p<0.05 and p<0.01.

3. Results and discussion

3.1. Global measurements

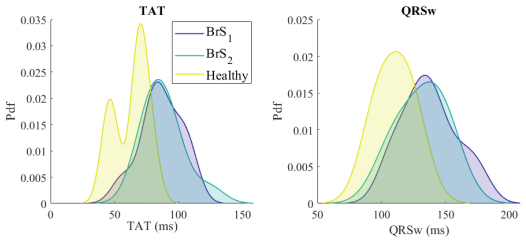

Figure 1. Probability density function (Pdf) of global measurements TAT and QRS_w. BrS_1 patients data are depicted in purple, BrS_2 in blue and controls in yellow.

Both BrS_1 and BrS_2 patients showed significantly wider QRS complexes compared with healthy controls (134 ±21 ms and 135±18 ms vs 116±12 ms, p<0.01) and longer TAT (86±16 and 82.9±13.5 vs 67±13 ms, p<0.01), as shown in Figure 1. No significant differences were observed between BrS_1 and BrS_2 groups.

3.2. Regional measurements

Examples of representative activation maps for each group are shown in Figure 2.

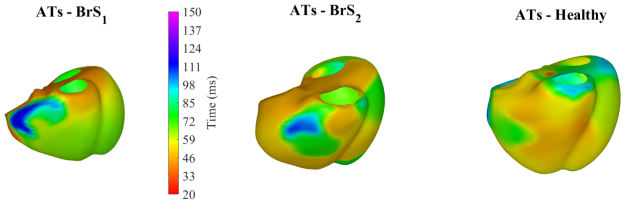

Figure 2. Representative activation maps for each group.

Analysis of AT_m revealed significant activation delays in the anterior RV, lateral LV, and medial LV segments in BrS_1 patients compared to healthy controls (p<0.05, Figure 3 Panel A). Notably, marked activation delays were observed in regions encompassing the RVOT as well as in multiple LV territories. Although not statistically significant in all regions, a general trend toward delayed epicardial activation was present in BrS_1 patients, except in the RV infero-basal segment, where controls displayed later activation. This reflects that, in healthy subjects, the RV infero-basal segment is typically the last to activate. The difference was not significant, as BrS patients also showed a delay in that area, although it was not their last area to activate (Figure 3 Panel B).

Maximum activation delays AT_{90} in the RVAB segment were significantly prolonged in BrS_1 patients compared to controls (BrS_1:103±21 ms vs Healthy: 64±14 ms, p < 0.01). Several LV segments also exhibited important activation delays in BrS_1 (especially in the inferior region, where delays in activation times were observed, p<0.01 in the apical segment). In contrast, the RV infero-basal segment tended to activate later in controls, although the differences did not reach statistical significance (66 ± 15 ms in BrS_1 vs 82 ± 15 ms in controls).

For minimum activation times AT_{10}, delays were evident in lateral LV and antero-medial RV segments in BrS_1, contributing to the prolongation of AT_m. The RVAB segment also showed delays with borderline statistical significance (46±10 ms in BrS_1 vs 40±6 ms in controls, p=0.05).

When comparing BrS_1 and BrS_2 (Figure 3 Panel C), BrS_1 epicardium was found to be delayed compared to BrS_2, except for some segments of the basal area.

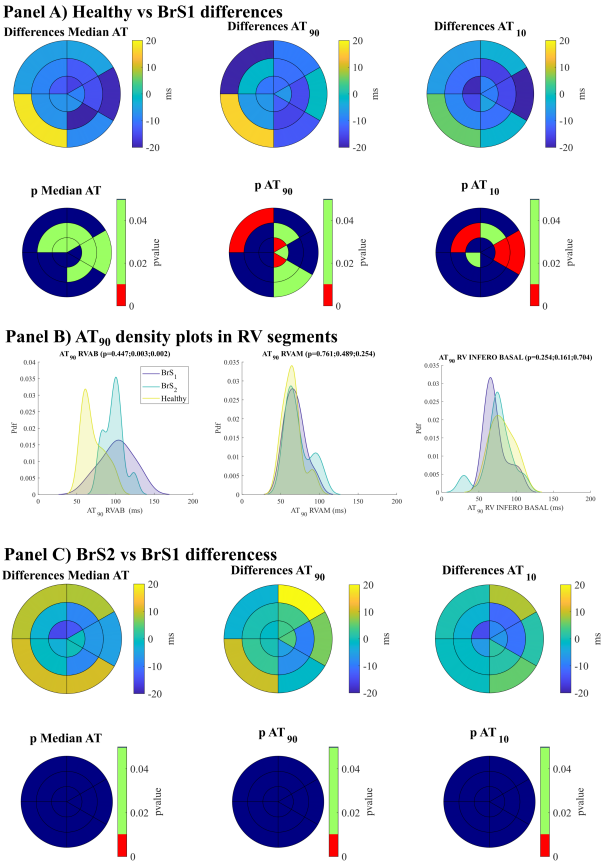

Figure 3. A) Differences between healthy controls and BrS_1 patients with corresponding p-values: dark blue higher values in BrS_1, yellow indicates higher values in controls. The lower row shows statistical significance (blue: non-significant, green: p<0.05, red: p<0.01). B) Probability density functions for RV segments. C) Comparison between BrS_1 and BrS_2 population: dark blue indicates higher values in BrS_1, yellow indicates higher values in BrS_2. The lower row displays p-values as in A.

No significant differences were observed in any segment in AT_m, AT_{10} or AT_{90} values. However, delay trends were present in BrS_1 with respect to BrS_2 in the latero-medial segment of the LV, reflecting borderline delayed activation onset and delayed AT_m, with AT_{10} values of 66±11 ms in BrS_1 vs 56±12 ms in BrS_2, p=0.068, and AT_m values of 72±10 ms in BrS_1 vs 67±11 ms in BrS_2, p=0.068. Analysis AT_{25} revealed significant differences, with AT_{25} values of 67±11 ms in BrS_1 vs 61±12 ms in BrS_2, p<0.05. Notably, no differences were found in RVOT activation between the two BrS groups, suggesting a more homogeneous conduction profile in this region. However, persistent intergroup differences in LV segments suggest that the BrS substrate extends beyond the RVOT, consistent with emerging evidence challenging the view of BrS as an isolated RVOT channelopathy [8], and instead impli-

cating broader electrical remodeling across both ventricles [9] [10].

4. Conclusion

BrS patients show delayed RVOT activation compared to healthy controls, consistent with impaired sodium channel function in this region. Spontaneous type 1 BrS patients display additional abnormalities beyond the RVOT, suggesting more extensive ventricular remodeling compared to drug-induced type 2 BrS patients. Validation in larger cohorts to increase the power of the statistical tests and confirm borderline results and tendencies is warranted, as these findings may improve risk stratification in BrS.

Acknowledgments

This work was supported by projects PID2021-128972OA-I00, PID2022-140556OB-I00, CNS2022-135899 and TED2021-130459B-I00 funded by MCIN/AEI /10.13039/501100011033 and "ERDF A way of making Europe", by fellowship RYC2019-027420-I funded by Ramón y Cajal Program and by BSICoS group T39_23R and project LMP94_21 funded by Aragón Government and FEDER 2014-2020 "Building Europe from Aragon". Computations were performed using ICTS NANBIOSIS (HPC Unit at U. Zaragoza).

References

[1] Brugada P. On Risk Stratification and its Paradoxes. European Heart Journal 11 2020;42(6):715–716.

[2] Tadros R, Nannenberg E, Lieve K, Alders M, Postema P, Caliskan K, Bhuiyan Z, Mannens M, Christiaans I, Bezzina C, Wilde. Yield and Pitfalls of Ajmaline Testing in the Evaluation of Unexplained Cardiac Arrest and Sudden Unexplained Death: Single-Center Experience With 482 Families. JACC Clinical Electrophysiology 12 2017; 3(12):1400–1408.

[3] Pannone L, Monaco C, Sorgente A, Vergara P, Calburean P, Gauthey A, Bisignani A, Kazawa S, Strazdas A, Mojica J, Lipartiti F, Housari MA, Miraglia V, Rizzi S, Sofianos D, Cecchini F, Osorio T, Paparella G, Ramak R, Overeinder I, Bala G, Almorad A, Stroker E, Pappaert G, Sieira J, Brugada P, Meir ML, Chierchia G, de Asmundis C. Ajmaline-Induced Abnormalities in Brugada Syndrome: Evaluation With ECG Imaging. Journal of the American Heart Association 2022;11(2):e024001.

[4] Isbister J, Strocchi M, Riedy M, Yeates L, Gray B, Singer E, Bagnall R, Ingles J, Raju H, Semsarian C, Niederer S, Sy R. Noninvasive Assessment of Hydroquinidine Effect in Brugada Syndrome (QUIET BrS). Heart Rhythm 2024;.

[5] Monaco C, Eltsov I, Monte AD, Aglietti F, Pannone L, Rocca DD, Gauthey A, Bisignani A, Mouram S, Calburean PA, Pappaert G, Bala G, Sorgente A, Almorad A, Stroker E, Sieira J, Sarkozy A, Chierchia GB, Meir ML, Brugada P, de Asmundis C. Assessment of Activation Delay in the Right Ventricular Outflow Tract as a Potential Complementary Diagnostic Tool for Brugada Syndrome. Europace 2025;27:euaf093.

[6] Kawada S, Morita H, Antzelevitch C, Morimoto Y, Nakagawa K, Watanabe A, Nishii N, Nakamura K, Ito H. Shanghai Score System for Diagnosis of Brugada Syndrome: Validation of the Score System and Reclassification of the Patients. JACC Clinical Electrophysiology 2018;4(6):724–730.

[7] Martínez J, Almeida R, Olmos S, Rocha A, Laguna P. A Wavelet-Based ECG Delineator Evaluation on Standard Databases. IEEE Transactions on Biomedical Engineering 4 2004;51:570–581.

[8] Oliva A, Grassi S, Pinchi V, Cazzato F, Coll M, Alcalde M, Vallverdu-Prats M, Perez-Serra A, Martinez-Barrios E, Cesar S, Iglesias A, Cruzalegui J, Hernandez C, Fiol V, Arbelo E, Diez-Escute N, Arena V, Brugada J, Sarquella-Brugada G, Brugada R, Campuzano O. Structural Heart Alterations in Brugada Syndrome: Is it Really a Channelopathy? a Systematic Review. Journal of Clinical Medicine 2022; 11(15):4406.

[9] Cheniti G, Haissaguerre M, Dina C, Kamakura T, Duchateau J, Sacher F, Racine HP, Surget E, Simonet F, Gourraud JB, Sridi S, Cochet H, Andre C, Bouyer B, Chauvel R, Tixier R, Derval N, Pambrun T, Dubois R, Jais P, Nademanee K, Redon R, Schott JJ, Probst V, Hocini M, Barc J, Bernus O. Left Ventricular Abnormal Substrate in Brugada Syndrome. JACC Clinical Electrophysiology 2023;9(10):2041–2051.

[10] Norihisa T, Morita H, Nagase S, Taniguchi M, Miura D, Nishii N, Nakamura K, Ohe T, Kusano K, Ito H. Atrial Electrophysiological and Structural Remodeling in High-Risk Patients with Brugada Syndrome: Assessment with Electrophysiology and Echocardiography. Heart Rhythm 2010;7(2):218–224.

Address for correspondence:

Inés Noguero Soler
University of Zaragoza, Campus Río Ebro, I+D Building, C/ Mariano Esquillor, s/n, D5.01.1B,
inoguero@unizar.es